ChemComm
Chemical Communications

Accepted Manuscript

This article can be cited before page numbers have been issued, to do this please use: M. Kaste, T. Heilmann, J. Kircher, C. Golz, R. A. Mata and M. Alcarazo, *Chem. Commun.*, 2026, DOI: 10.1039/D5CC07240A.

ROYAL SOCIETY OF CHEMISTRY

rsc.li/chemcomm

ChemComm

View Article Online
DOI: 10.1039/D5CC07240A

COMMUNICATION

Synthesis and Reactivity of a Strongly Pyramidalized P(III)-Compound Embedded into a Pyrrolide $(ONO)^{3-}$ Pincer Ligand

Received 00th January 20xx,
Accepted 00th January 20xx

DOI: 10.1039/x0xx00000x

Malte Kaste,[a,†] Tobias Heilmann,[a,†] Johannes Kircher,[b] Christopher Golz,[a] Ricardo A. Mata[b] and Manuel Alcarazo[a,*]

A C_s-symmetric P(III) complex bearing a pyrrolide-centered trianionic pincer ligand is reported and its reactivity explored. This compound reacts with alcohols and amines *via* oxidative addition of their respective O-H and N-H bonds at the P-center, delivering the corresponding P(V) species. DFT calculations, as well as kinetic and isotope labelling analyses suggest the assistance of one of the phenolate side arms in the process.

The embedment of a formal tricationic P-centre into the rigid environment created by pincer ligands is known to deliver geometrically distorted phosphabicyclic compounds that are characterized by unique electronic structure and reactivity.[1,2,3,4] For instance, compound **A** is a competent catalyst for transfer hydrogenation reactions,[5] while **B** undergoes E-H activation reactions (E = -OR, -NHR, BR_2);[6] mimicking in both cases the behavior of transition metal complexes in small molecule activation processes. The origins of this specific reactivity lie in the decreased HOMO-LUMO gap when compared with their undistorted C_{3v}-symmetric congeners, which is caused by the imposed non-trigonal geometries and facilitates oxidative addition reactivity. Moreover, alternative activation pathways based on the cooperation of the P-center with the flanking ligand might also get involved.[7] Considering the key role played by the pincer framework to finely tune and leverage these reactivity modes, it is not surprising that during the last years a number of tri- and dianionic scaffolds containing ONO,[5,8,9] NNN,[6,10,11,12] NPN,[13] OCO,[14] CNC[15] or ONP[16] donor sites have been evaluated among others.[17,18,19] They afford neutral (**A-E**) or cationic species (**F-I**),[20] respectively; each one depicting unique modes of reactivity (Figure 1a).

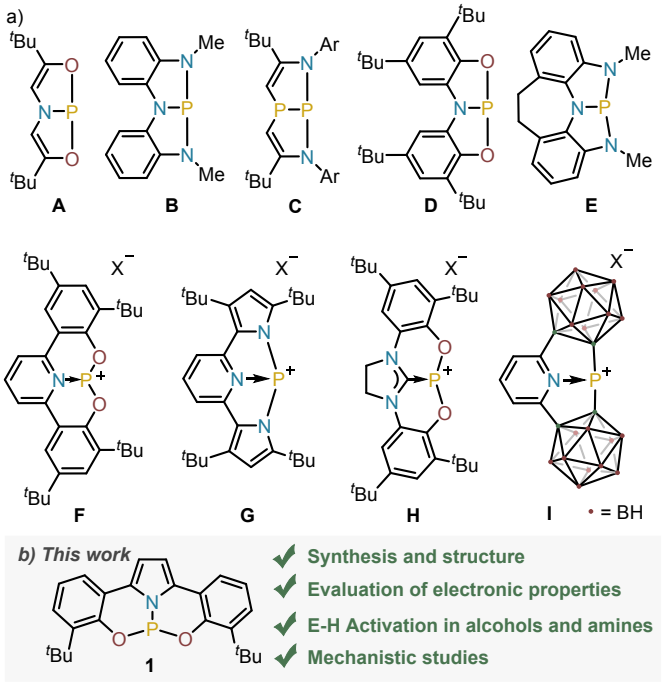

Figure 1 (a) Selection of previously studied constrained P(III)-species; (b) This work: a P(III)-compound embedded into a pyrrolide $(ONO)^{3-}$ pincer ligand.

Some years ago, Veige described a new trianionic pyrrolide containing pincer ligand **2**,[21] which has been used for the synthesis of W, Ti and Zr complexes (Scheme 1).[22] During these studies the ability of the pyrrolide moiety to undergo reversible remote protonation at the backbone was noticed. This unusual behaviour motivated us to study whether its P-derivative **1** might also undergo E-H activation processes (E = -OR, -NHR) through a cooperation mode that involves the P-center and the remote 3-position of the pyrrolide ligand.

[a]*Institut für Organische und Biomolekulare Chemie, Georg-August-Universität Göttingen. Tammannstr. 2, 37077 Göttingen, Germany.*
E-mail: manuel.alcarazo@chemie.uni-goettingen.de
[b]*Institut für Physikalische Chemie, Georg-August-Universität Göttingen Tammannstr. 6, 37077 Göttingen, Germany.*
† Equal contribution from both authors
Electronic Supplementary Information (ESI) available: [details of any supplementary information available should be included here]. See DOI: 10.1039/x0xx00000x

Hence, phosphine **1** was prepared by treatment of **2** with PCl_3 in the presence of slight excess of Et_3N (3.5 equiv.). The ^{31}P NMR spectrum of the reaction crude showed a well-defined signal at 114.7 ppm, which closely matches the values reported for highly pyramidalized **F** (117 ppm in CD_2Cl_2)[9] or **G** (112 ppm in $CDCl_3$).[11] Subsequent evaporation of the solvent and crystallization from *n*-pentane afforded analytically pure **1** as pale-yellow needles (86% yield), which were used to determine its molecular structure by X-ray crystallography (Scheme 1b). In the solid state **1** depicts strong pyramidalization at the P-centre ($\sum_{<P}$= 288°); comparable **F**($\sum_{<P}$= 286°) and **G**($\sum_{<P}$= 293°). Both P-O bond lengths (1.635(1)Å and 1.631(1)Å) fall within the expected range for P(III)-O bonds, while the P-N bond length in **1** (1.704(1)Å) is significantly shorter than that in cationic **F** (1.809(2)Å) or even the neutral phosphoramidite **D** (1.757(1)Å).[8]

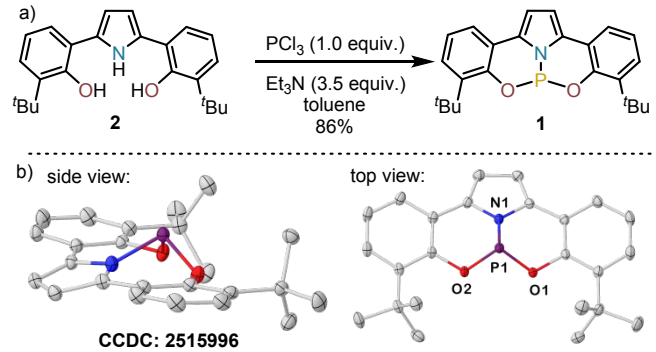

Scheme 1 (a) synthesis of **1**; (b) Structure of **1** in the solid state.

Willing to obtain some evidence about the impact that the distortion provoked by the pincer ligand generates on the electronic properties, we decided to assess the donor strength of **1** by IR spectroscopy, using the cyclopentadienyliron dicarbonyl cation $[Fe(CO)_2]^+$ as probe. The IR spectrum of **3** shows two CO stretching vibrations ($\tilde{\upsilon}_{asym}$ = 2030 cm^{-1} and $\tilde{\upsilon}_{sym}$ = 2073 cm^{-1}), which are higher in energy than that of the analogue phosphoramidite complex **6**, and better align the donor properties of **1** with these of phosphites **4-5**, (Figure 2a).[23,24,25] A substantial decrease of the donor ability upon distortion is observed by comparison of **7** and **8**;[26] an effect that probably also plays a role in **3** (when compared to **6**). The qualitative trend is also corroborated by the J_{PSe} coupling constant in **9** ($J_{P\text{-}Se}$ = 1018 Hz), which is significantly higher than that of **10** or **11**, and indicates that **1** is a weaker donor than of $P(OMe)_3$ or $(Me_2N)P(OMe)_2$ (Figure 2b).[27] Calculations at the B3LYP-D3(BJ)/def2-TZVP theory level support this conclusion.[28] They reveal a LUMO substantially lower in energy than that for non-constrained analogues, which is expected to confer enhanced Lewis acidity at the P-atom. It also suggests its possible involvement in E-H bond activation processes (see Figures S17-S18 for details).

The redox chemistry of **1** was subsequently studied by cyclic voltammetry (CV). Its voltammogram shows a quasi-reversible wave with an oxidation potential of E^{ox} = 0.69 V *vs*. $Fc^{0/+}$. In agreement with that value, addition of magic blue to a CH_2Cl_2 solution of **1** at -78°C resulted in the development of an intense green colour. The recorded X-band isotropic spectrum of the newly generated species, which we assume to be $\mathbf{1}^{+\bullet}$, has been simulated with a g value of 2.003 and hyperfine constants of 1.66 G to the central ^{31}P(I =1/2), 0.98 G to the pyrrolic ^{14}N(I=1), and 4.32 G, 2.67 G and 2.13 G to three pairs of protons 1H(I=1/2) (Figure 2e). The calculated SOMO of $\mathbf{1}^{+\bullet}$ is mainly delocalized over the pincer ligand, with Mulliken spin densities of 13.7% and 7.0% at the *p*-C and *o*-C of the phenolate units, respectively; 5.7% at each backbone carbon of the pyrrolide moiety, 5.5% at the N atom and only 0.3% at P (Figure 2f).

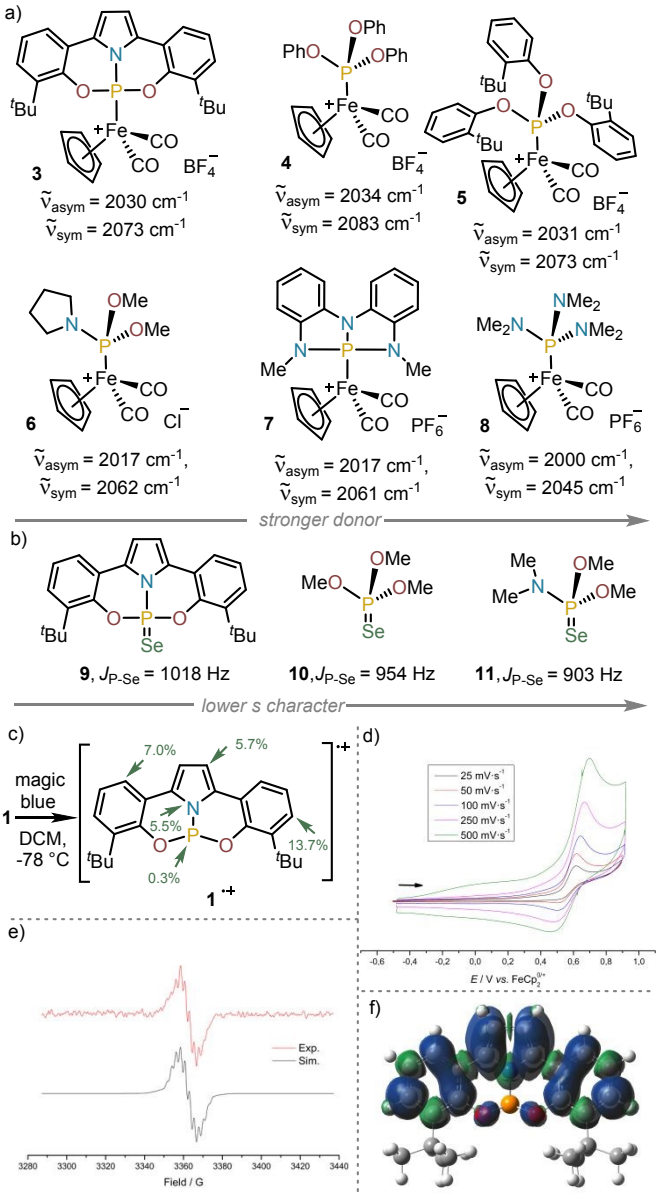

Figure 2 Evaluation of the donor properties of **1**: (a) IR stretching frequencies of L[CpFe(CO)$_2$] complexes; (b) J_{PSe} of model phosphorous selenides; (c) Synthesis of $\mathbf{1}^{+\bullet}$; (d) CV of **1**; (e) EPR spectrum of $\mathbf{1}^{+\bullet}$; (f) SOMO of $\mathbf{1}^{+\bullet}$.

Having synthesized and characterized **1**, the screening of its ability to activate the N-H bond of amines started. Exposure of **1** to stoichiometric amounts of primary amines (butyl-, benzyl-, isobutyl- and neopentyl-) in chloroform at room temperature led to quantitative consumption of **1** and the clean formation of the corresponding hydridoamidophosphorane, which are

characterized by high field resonances in the ^{31}P NMR spectra (δ= -80 -(-90)ppm), and large $^{1}J_{P\text{-}H}$ coupling constants ($^{1}J_{P\text{-}H}$ =848-865 Hz), indicating pentacoordination of the P-atom and the formation of a P-H bond (For details see the ESI). Bulkier amines such as isopropyl- and tertbutyl amines, or less nucleophilic anilines required longer reaction times and the reaction mixtures to be heated to 60 °C to ensure complete conversion (Scheme 2a). The formation of compounds of general formula **12** is a reversible process; for example, by heating **12b** at 120°C under vacuum (10^{-3} bar) **1** is recovered.[19,29] In addition, heating **12c** with an excess of i-$BuNH_2$ (5.0 equiv.) leads to amine exchange. Finally, reaction of **1** with deuterated isobutylamine afforded **12b-*d*$_2$** (^{31}P NMR δ= -84.7 ppm, $^{1}J_{P\text{-}D}$ = 129.4 Hz). No deuterium label was detected at the pyrrolide backbone *via* ^{2}H NMR analysis, ruling out the involvement of that site during the N-H activation process

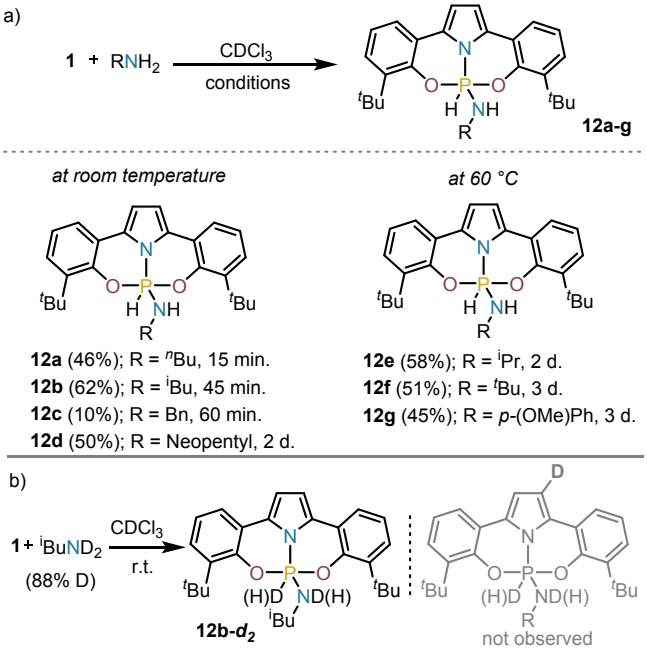

(Scheme 2b).

Scheme 2 (a) N-H oxidative addition products **12a-g**; (b) preparation of deuterium labelled **12b-*d*$_2$**. Complete conversions were achieved. Yields are of the isolated products.

Compound **12d** has been crystallized from *n*-pentane and its structure is depicted in Figure S14. When compared with **1**, the structure of **12d** exhibits slight elongation of the P-O bond lengths (P1-O1, 1.685(1)Å and P1-O2, 1.713(1)Å), while the P1-N1 (1.700(1)Å) remains unchanged within the error range. Moreover, the pentacoordinate phosphorus atom adopts a nearly undistorted trigonal bipyramidal geometry (τ_5 = 0.97).[30] Kinetic studies have been undertaken by monitoring the formation of phosphorane **12d** *via* ^{1}H NMR spectroscopy during 12 hours. Tetrakis(trimethylsilyl)silane was employed as standard and the temperature was kept constant at 25 °C. Under these conditions the orders in **1** and amine have been determined to be 1.0 in both cases using a variable time normalization analysis (VTNA) (Figures S7-11).[31,32,33]

Next, the reactivity of **1** with alcohols was evaluated. No reaction was observed when MeOH, EtOH or PrOH were added to solutions of **1** in $CHCl_3$; yet, the activation of the O-H bond slowly occurs if an acid catalyst ($[HOEt_2][B(C_6H_3(CF_3)_2)_4]$; 10 mol%) is present in the reaction mixture delivering compounds **13a-e**(Scheme 3a). This observation suggests that an initial protonation of **1** is necessary to boost reactivity. To evaluate this hypothesis **1** was exposed to CD_3OD under acidic conditions, and the incorporation of the isotope label determined by multinuclear NMR. In **13a-*d*$_4$** deuterium was found statistically distributed among the two positions of the pyrrolide backbone and the P-centre (Scheme 3b). This observation suggests an active participation of the pyrrolide moiety in the activation process. Most probably, the protonation of **1** at the pyrrole backbone generates a phosphenium cation of enhanced Lewis acidity, which is more capable of coordinating the alcohol substrate at P; thus, initiating the activation process.[9,11,13] Yet, protonation at phosphorus followed by attack of the alcohol cannot be excluded. In that case, the H/D exchange at C3 of the pyrrole should occur after the formal oxidative addition step.[21,22]

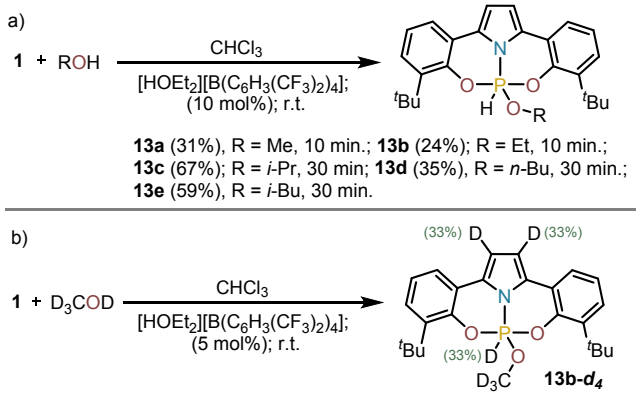

Scheme 3 (a) O-H oxidative addition products **13a-e**; (b) Incorporation of the deuterium label in the ONO supporting ligand; Complete conversions were achieved. Yields are of the isolated products.

To get deeper insight into the mechanism leading to the formation of hydridoamidophosphoranes **12**, the reaction pathway was evaluated through computational methods. The reaction intermediates and selected transition states were optimized at the B3LYP D3(BJ)/def2-TZVP level of theory, making use of the D3 Grimme dispersion correction with Becke-Johnson damping.[34] Solvation effects were accounted through single point corrections using the SMD model and chloroform as solvent at the B3LYP-D3(BJ)/def2-TZVP level.[35] The structure of transition state **TS4** was obtained via the nudged-elastic band method.[36]

Our calculations indicate that at the very first step the amine coordinates the phosphorous atom through **TS1**. Subsequent shuttle of a proton from the amine moiety in **Int1** to the oxygen atom of the neighbouring phenolate ligand with concomitant P-O bond cleavage delivers **Int2** (Figure 4). From this point, the system evolves to **Int3** via rotation of the phenolate ligand, and finally, the proton is transferred to the P-atom via **TS4**. Considering the uncertainty associated with the DFT computed

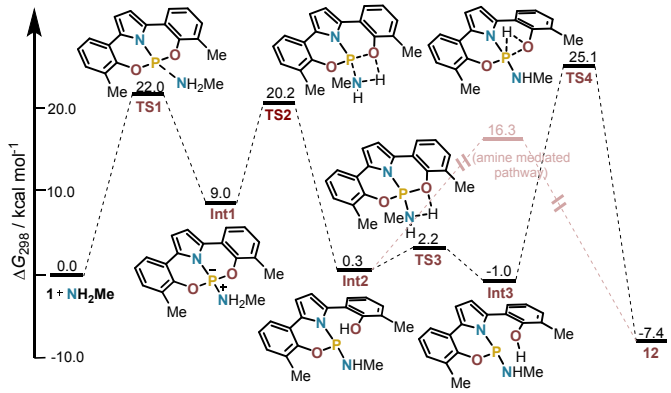

Figure 3: Free energy profile for the reaction of **1** with methylamine calculated at the B3LYP-D3(BJ)/def2-TZVP(SMD)//B3LYP-D3(BJ)/def2-TZVP level of theory. *tert*-Bu groups were replaced by methyl groups for these calculations.

barriers and the relatively small energetic difference between **TS1** and **TS4** (22.0 and 25.1 kcal/mol, respectively), both steps are potentially rate-determining. However, independent of where the bottleneck is, the reaction rate should still be first-order with respect to the reacting phosphine and amine. If **TS1** is the rate-limiting step, this follows immediately. If **TS4** is rate-limiting, an effective first order rate constant with respect to both reagents can be deduced assuming **1** and the amine to be in chemical equilibrium with **Int3** (See the ESI for the analysis). Finally, we have also considered that proton transfer from **Int2** to **12** could be assisted by amine through a hydrogen bond network. This pathway requires a series of elementary steps but proceeds through a much lower barrier (16.0 kcal/mol; Figure S20). In this scenario, which might be operative at an initial stage of the reaction, **TS1** is clearly rate determining.

In conclusion, we describe herein the synthesis of a structurally distorted P(III)-complex stabilized by a pyrrolide $(ONO)^{3-}$ pincer ligand and preliminarily discuss its oxidation and coordination chemistry. Compound **1** readily react with amines to deliver the corresponding hydridoamidophosphoranes, and theoretical calculations indicate that the operative pathway involves the cooperation between the P-centre and a phenolate arm. Contrarily, the oxidative addition of alcohols requires the intervention of a Brønsted acid catalyst to proceed. Deuterium labelling experiments suggest that in such reactions a phosphenium cation of enhanced Lewis's acidity is formed by protonation of the pyrrolide backbone. This cationic species is the one that presumably initiates the O-H oxidative addition by coordination of the alcohol substrate to the electrophilic P-centre.

M. A. conceived and coordinated the project. M. K. and T. H. performed the experiments. M. K, J. K and R. A. M. carried out the computational studies. C. G. did the X-ray crystallographic studies. M. K., R. A. M. and M. A. prepared the manuscript. All authors discussed the results.

This work was supported by the Deutsche Forschungs-gemeinschaft (DFG) through the BENCh Research Training Group 389479699/GRK2455 and projects INST 186/1318-1 and INST 186/1324-1.

Conflicts of interest

There are no conflicts to declare.

View Article Online
DOI: 10.1039/D5CC07240A

Data availability

Further details of the experimental procedures, NMR spectra, and DFT data are available in the ESI.†. CCDC numbers 2515996 and 2515997 contain supplementary crystallographic data for **1** and **12d**, respectively.

Notes and references

1 S. Kundu, *Chem. Asian J.* 2020, **15**, 3209-3224.
2 J. Abbenseth, J. M. Goicoechea, *Chem. Sci.* 2020, **11**, 9728-9740.
3 A. Maiti, R. Yadav, L. Greb, Structural constraint effects on p-block elements: Recent advances, chapter 8, *Adv. Inorg. Chem*. 2023, **83**, 261-299.
4 T. J. Hannaha, S. S. Chitnis, *Chem. Soc. Rev.* 2024, , 764-792.
5 N. L. Dunn, M. Ha, A. T. Radosevich, *J. Am. Chem. Soc.,*2012, **134**, 11330-11333.
6 (a) W. Zhao, S. M. McCarthy, T.-Y. Lai, H. P. Yennawar, A. T. Radosevich, *J. Am. Chem. Soc.,* 2014, **136**, 17634-17644; (b) Y.-C. Lin, E. Hatzakis, S. M. McCarthy, K. D. Reichl, T.-Y. Lai, H. P. Yennawar, A. T. Radosevich, *J. Am. Chem. Soc.,* 2017, **139**, 6008-6016.
7 J. M. Lipshultz, G. li, A. T. Radosevich, *J. Am. Chem. Soc.* 2021, **143**, 1699-1721.
8 T. P. Robinson, D. M. de Rosa, S. Aldridge, J. M. Goicoechea, *Angew. Chem. Int. Ed.*, 2015, **54**, 13758-13763.
9 S. Volodarsky, R. Dobrovetsky, *Chem. Commun.*, 2018, **54**, 6931-6934.,
10 H. W. Moon, A. Maity, A. T. Radosevich, *Organometallics,* 2021, **40**, 2785-2791.
11 S. Volodarsky, D. Bawari, R. Dobrovetsky, *Angew. Chem. Int. Ed.,* 2022, **61**, e202208401.
12 A. J. King, J. Abbenseth, J. M. Goicoechea, *Chem. Eur. J.* 2023, **29**, e202300818.
13 J. Cui, Y. Li, R. Ganguly, A. Inthirarajah, H. Hirao, R. Kinjo, *J. Am. Chem. Soc.,* 2014, **136**, 16764-16767.
14 D. Bawari, I. Malahov, R. Dobrovetsky, *Angew. Chem. Int. Ed.,* 2025, **64**, e202419772.
15 D. Bawari, D. Toami, K. Jaiswal, R. Dobrovetsky, *Nat. Chem.* 2024, **16**, 1261-1266.
16 L. You, D. Roth, L. Greb, *Chem. Sci.*, 2025, **16**, 1716-1721.
17 A. Brand, A. Hentschel, A. Hepp, W. Uhl, *Eur. J. Inorg. Chem.* 2020, 361-369.
18 D. Roth, A. T. Radosevich, L. Greb, *J. Am. Chem. Soc.* 2023, **145**, 24184-24190.
19 J. Abbenseth, O. P. E. Townrow, J. M. Goicoechea, *Angew. Chem. Int. Ed.* 2021, **60**, 23625-23629.
20 For a recent review see: D. Bawari, D. Toami, R. Dobrovetsky, *Chem. Commun.* 2025, **61**, 5871-5882.
21 M. E. O'Reilly, S. S. Nadif, I. Ghiviriga, K. A. Abboud, A. S. Veige. *Organometallics*, 2013, **33**, 836-839.
22 S. S. Nadif, M. E. O'Reilly, I. Ghiviriga, K. A. Abboud, A. S. Veige, *Angew. Chem. Int. Ed.,* 2015, **54**, 15138-15142.
23 H. Schumann, *J. Organomet. Chem.* 1985, **293**, 75-91.
24 H. Nakazawa, Y. Kadoi, K. Miyoshi, *Organometallics* 1989, **8**, 2851-2856.
25 N. Nakazawa, K. Kubo, K. Tanisaki, K. Kawamura, K. Miyoshi, *Inorg. Chim. Acta*, 1994, **222**, 123-129.
26 G. T. Cleveland, A. T. Radosevich, *Angew. Chem. Int. Ed.* 2019, **58**, 15005-15009.

View Article Online
DOI: 10.1039/D5CC07240A

27 D. E. Schiff, J. W. Richardson, R. A. Jacobson, A. H. Cowley, L. Lasch, *Inorg. Chem.* 1984, **23**, 3373-3377.
28 A. D. Becke, *J. Chem. Phys.* 1993, **98**, 5648-5652.
29 N. Beims, T. Greven, M. Schmidtmann, J. I. van der Vlugt, *Chem. Eur. J.* 2023, **29**, e202302463.
30 A. W. Addison, N. T. Rao, J. Reedijk, J. van Rijn, G. C. Verschoor, *J. Chem. Soc., Dalton Trans.* 1984, **7**, 1349–1356.
31 J. Burés, *Angew. Chem. Int. Ed.* 2016, **55**, 2028-2031.
32 J. Burés, *Angew. Chem. Int. Ed.* 2016, **55**, 16084-16087.
33 C. D.-T. Nielsen, J. Burés, *Chem. Sci.* 2019, **10**, 348-353.
34 S. Grimme, S. Ehrlich, L. Goerigk, *J. Compt. Chem.,* 2021, **32**, 1456-1465.
35 F. Weigend, R. Ahlrichs, *Phys. Chem. Chem. Phys.,* 2005, **7**, 3297-3305.
36 O. Weser, B. Hein-Janke, R. A. Mata, *J. Comp. Chem.,* 2023, **44**, 710-726.

View Article Online
DOI: 10.1039/D5CC07240A

Data availability

Further details of the experimental procedures, NMR spectra, and DFT data are available in the ESI.†. CCDC numbers 2515996 and 2515997 contain supplementary crystallographic data for **1** and **12d**, respectively.